Tribology and Materials
Vol. 1, No. 2, 2022, pp. 42-54

ISSN 2812-9717
https://doi.org/10.46793/tribomat.2022.007

Simulation of heat transfer in a turbocharger bearing housing

Elena ZADOROZHNAYA [1], Vlad HUDYAKOV [1,*], Sergey SIBIRYAKOV [2]

[1] Department of Automobile Transport, South Ural State University, Chelyabinsk, Russia
[2] JSC "TURBOCOMPLEKT", Protvino, Russia
*Corresponding author: introfollow@yandex.ru

Keywords
turbocharger
heat transfer
CFD
journal bearing
rotor dynamics

History
Received: 11-04-2022
Revised: 11-05-2022
Accepted: 14-05-2022

Abstract

Modern world trends in engine building are characterised by the production of forced engines. The most popular and promising forcing method is the use of a turbocharger. The efficiency of journal bearings determines the reliability of TCR, which should be structurally simple, compact, reliable and inexpensive, while providing acceptable characteristics of rotor dynamics, noise, vibration and stiffness speeds. The best performance of the bearing unit is achieved with hydrodynamic lubrication, which depends on optimal operating and temperature conditions. The maximum operating temperature of the bearing assembly must be taken into account at the design stage. The purpose of this article is to develop an algorithm for calculating the heat transfer in the turbocharger bearing housing in order to assess the effect of the thermal state of the radial bearing on its performance and on the dynamics of the rotor. The simulation was carried out in the ANSYS software package and the developed software. The boundary conditions for the calculation were obtained from experimental data. The result of the simulation was the determination of temperatures and thermal fields in the turbocharger housing, as well as the values of the change in clearances under the influence of thermal expansion of parts. Verification of the results was carried out on the basis of comparison with the results obtained by other authors. Conclusions were drawn about the effect of thermal deformations on the rotor dynamics and the hydromechanical characteristics of the bearing.

1. Introduction

In the modern world, cars have become an integral part of everyday life. As the world population increases, so does the demand for cars. Modern internal combustion engines are characterised by high efficiency and environmental performance. The above factors can be realized through the use of a turbocharger (TCR).

The turbocharger is an indispensable element of a modern internal combustion engine, allowing to improve its performance. The prospects for the use of turbocharging can be traced to the growth of the world TCR market. In 2019, it was estimated at $16.13 billion, and according to experts, by 2027 it will reach $24.23 billion [1]. Turbochargers require no energy source other than exhaust gases and have found their way across a wide range of industrial sectors.

The operating conditions of turbochargers are inextricably linked with high values of pressure and temperature of exhaust gases (on average 800 – 1000 °C, depending on the type of engine), high rotation speed and variable dynamic loads acting on the rotor [2]. Based on the given number of reasons, the TCR elements are exposed to high a mechanical and thermal loads, which has a significant impact on their operation.

According to statistics from one of the market leaders, Garett – Advancing Motion, more than 90 % of turbocharger failures are associated with oil starvation, lubricant contamination and surface damage by foreign objects. Less than 1 % of turbine failures are due to factory defects, and the remaining percentage is due to improper operating

conditions [3]. Focusing on the main causes of turbocharger malfunctions, it becomes clear that the efficiency of the oil system and the support units that depend on it determine the reliability of the turbocharger. In a turbocharger, the role of support units is played by hydrodynamic journal bearings, which perceive radial and axial loads.

The operational characteristics of tribo-units largely depend on the quality of the lubricant and temperature conditions. Excessive temperatures in the bearing assembly contribute to accelerated oil oxidation, deterioration of its lubricating properties [4] and the formation of coke deposits. Coke deposits can clog bearing clearances and oil lines [5], leading to interruptions in the lubricant supply and, in the worst case, to oil starvation. It should be borne in mind that these deposits can move as particles through the lubrication system. When their concentration exceeds a certain value, the particles turn into an effective abrasive, which leads to damage to the friction surfaces and the violation of gaps [2]. The above factors lead to rotor failure due to seizure. The main types of turbocharger malfunctions are shown in Figure 1.

In recent years, the number of works devoted to unstable vibrations caused by uneven heating of the rotor has been growing [6-8]. The thickness of the lubricating layer differs depending on the local area, due to which the values of hydraulic losses differ. Where the layer thickness is less, there will be an increased hydraulic loss, which leads to uneven heating. Uneven heating causes thermal bending of the rotor, increasing its initial imbalance. This phenomenon is called the “Morton Effect”. The effect is difficult to recognize in practice, due to the difficulty of measuring the temperature distribution over the surface of the rotor, so modelling this phenomenon is an urgent task.

Many works are devoted to hot stops of the engine, which reduce the service life of the turbochargers [2,9,10]. With a sharp shutdown of the engine, the lubricant stops flowing into the journal bearings, and the parts do not have time to cool. Because of this, dry friction occurs between the bushing and the rotor. In particular, seals wear out, which leads to leakage of lubricant into the engine intake system. A hot stop of the engine leads to clogging of the bearing system with carbon deposits. The problem of hot stops is solved by using a turbo timer and a hydraulic accumulator [11].

Based on the analysis of scientific research, it can be concluded that modelling heat flows in a turbocharger and its elements is an urgent task. The thermal state of the TKR elements affects many of its characteristics: energy efficiency, environmental friendliness, reliability, hydromechanical characteristics of support units, rotor imbalance, rotor oscillation amplitudes, etc. Therefore, it is necessary to take into account the phenomenon of heat transfer already at the design stage of the TCR.

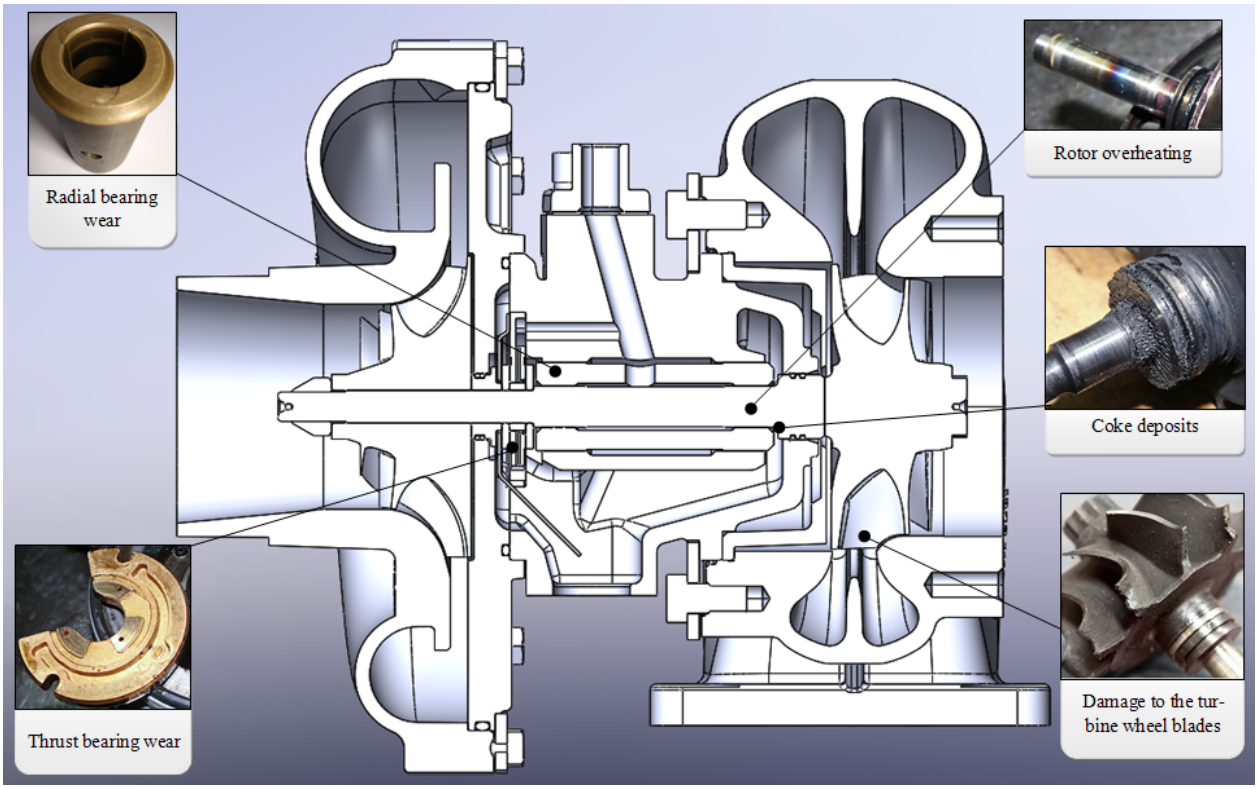

Figure 1. The main types of turbocharger malfunctions

Modelling heat flows in objects with complex geometry is a difficult task. Despite the complexity, many authors are trying to create perfect numerical models for calculating temperature values in different zones of a turbocharger [4,12-15].

Researchers from Hanover [16] conducted a simulation of the heat transfer process occurring in the TCR rotor. The work used diabatic and bidirectional approaches. An analysis of the heat transfer processes of the rotor shows that they change significantly if the influence of tribo-couples is taken into account. In the turbine side journal bearing, a significant amount of heat is removed from the rotor through the lubricant flow and leaves the system through convective heat exchange. In addition, heat is supplied to the rotor by both the compressor-side radial bearing and the thrust bearing, since energy dissipation in the lubricant causes corresponding temperature gradients.

Li et al. [17] in their work, they conducted experiments and numerical simulations to study the thermohydrodynamic characteristics of the turbocharger rotor bearing system. The temperature of the lubrication system and the vibration of the rotor were predicted by numerical simulation and confirmed experimentally. The results confirm that solid parts play a significant role in thermal load analysis as the temperature fields of solid parts affect oil film gaps due to thermal expansion. The rotor transfers a significant amount of heat from the turbine to the inner lubrication layer, and then a large amount of heat will be continuously transferred from the inner layer to the outer one through the sleeve.

Suvorov and Berdnikov [18] studied the optimisation of the shape of the rotor recess. The optimal recess shape made it possible to reduce the temperature in the investigated area, as well as to significantly reduce the values of the mass-inertial parameters. Due to this, the durability of the bearing assembly is increased, and the working characteristics of the TKR are improved.

Research [6] is devoted to the study of the influence of the thermal imbalance of the rotor on the oscillation amplitudes of the turbine generator bearings. The temperature difference causes a thermal bending of the rotor, which is converted into a thermal imbalance. The vibrations of the rotor are formed from mechanical and thermal imbalance, so the increase in temperature adversely affects the amplitude of the oscillations. Reducing the initial (mechanical) imbalance allows the reduction of vibration of the rotor and the temperature difference around the circumference of the trunnion because the temperature difference around the circumference of the rotor occurs due to viscous shear in the lubricating layer with a large amplitude of rotor oscillations).

The work of Aghaali et al. [19] is dedicated to an experimental study to analyse the different heat transfer conditions in a turbocharger. The results showed that the internal heat transfer from the turbine to the bearing housing is greater than the external heat transfer from the compressor to the bearing housing. The heat flux from the turbine was influenced by the gas temperature at the inlet to the turbine casing, the oil temperature, the heat flux of the coolant, and the airflow around the casing [20].

The article [21] presents a new method for quantifying transient heat transfer coefficients on moving surfaces of rotating bearings, based on infrared thermography. Experimental data is used as input to a heat transfer algorithm that quantifies the heat transfer coefficient. The use of transient temperature fields significantly reduces the study time from several hours to several minutes. The results of numerical simulations using the inverse algorithm show a good correlation with the experiment. The method is able to fix the change in the heat transfer coefficient with a change in the rotation speed, which was impossible to do with the previously existing methods.

Romagnoli et al. [22] conducted a detailed review on how to tackle TCR heat transfer through cutting edge research. Particular attention is paid to modern trends in solving this problem, which should be emphasized in the coming years.

Based on the foregoing, it can be concluded that modelling heat flows in turbocharger housing is an urgent and unsolved problem. The purpose of this article is to develop a methodology and algorithm for calculating heat transfer in the bearing housing of a turbocharger in order to assess the effect of the thermal state of the TKR radial bearing on its performance and the rotor dynamics. Analysis of the thermal state will improve the parameters of the durability and reliability of the rotor bearing assembly and the turbocharger as a whole.

2. Modelling method

2.1 Geometry

For numerical simulation, the geometry of the turbocharger (Fig. 2) manufactured by JSC “TURBOCOMPLEKT” was used.

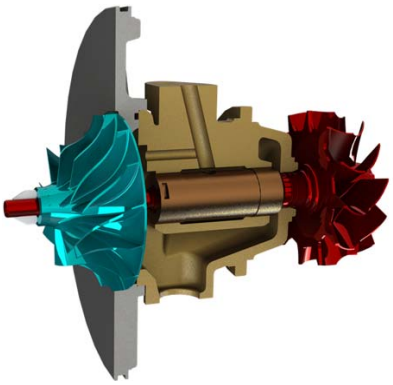

Working angular speed of rotation, rpm	95000
Rotor journal diameter, mm	14
Internal diameter clearance, μm	30
External diameter clearance, μm	60

Figure 2. Turbocharger by JSC "TURBOCOMPLEKT"

2.2 Calculation of gas dynamic processes

The first step in numerical modelling is the creation of a mesh model. The implementation of a high-quality mesh model is a stumbling block in solving many problems with complex geometry. For the wheels of the turbocharger, two mesh models were created, consisting of elements of a tetrahedral shape. These models had a large number of elements, so it was decided to convert the tetrahedral mesh to a polyhedral mesh. This allowed us to significantly reduce the number of cells and slightly increase their orthogonal quality. Thus, it turned out to reduce the time spent on the calculation and improve the convergence of the solution. The mean orthogonality was about 0.75. Cells with a quality criterion below the recommended value (0.01) were absent. Figure 3 shows a comparison of mesh models with different cell shapes.

The calculation of the gas dynamics of the turbine compressor impellers was carried out in the ANSYS Fluent software package. Experimental data obtained at the stand [23] were used as boundary conditions. The speed range varied from 48000 to 95000 rpm. Boundary conditions for calculating the turbocharger impellers are presented in Table 1.

Regardless of the type of fuel, most of the exhaust gases are nitrogen (74 – 78 %) [24]. Therefore, flue gases at a pressure of 1 atm were chosen as the working substance of the turbine, where the share of N_2 = 76 %, CO_2 = 13 % and H_2O = 11 % [25]. The working substance of the compressor is dry air at a pressure of 1 atm [25]. The properties of exhaust gases and dry air are presented in Tables 2 and 3.

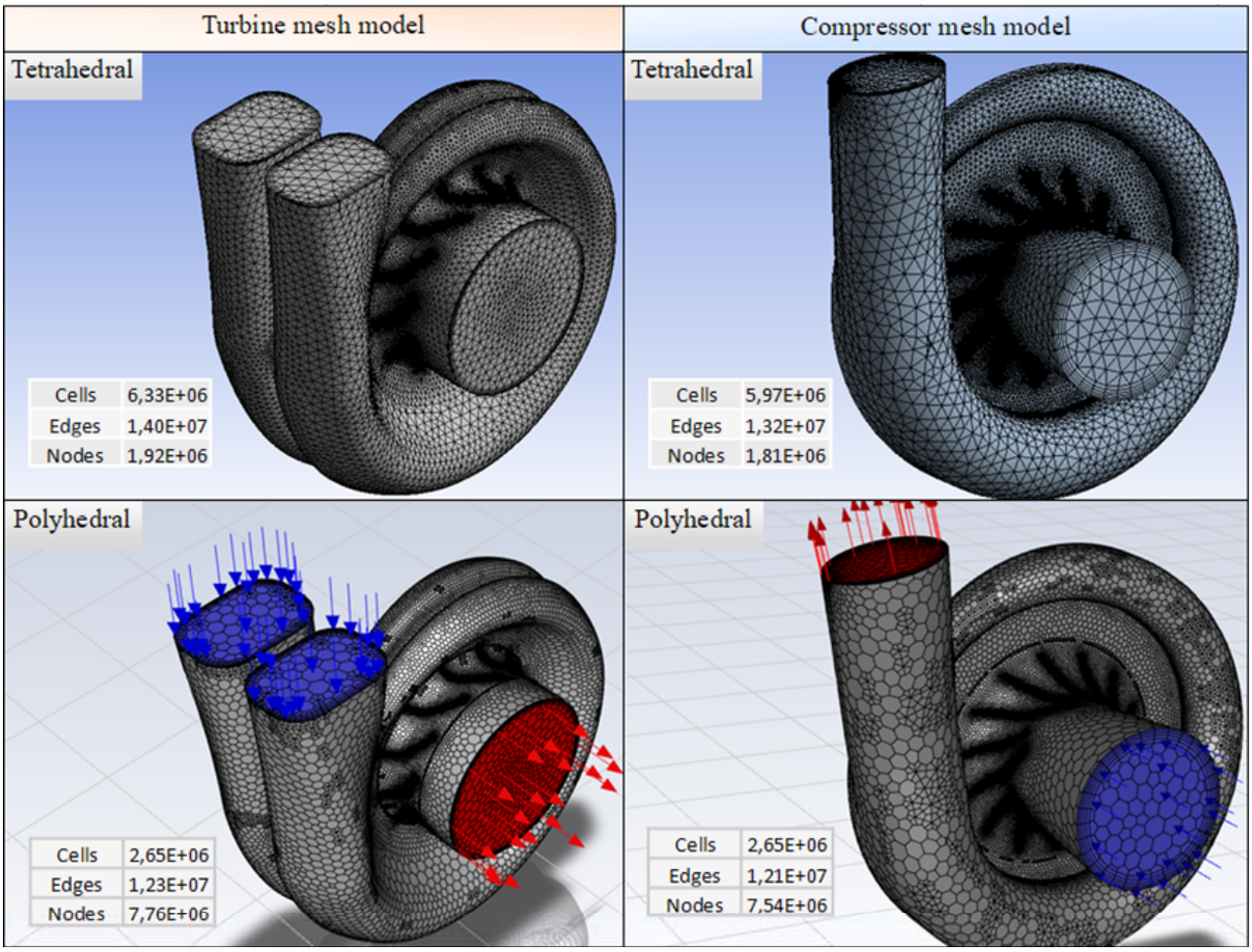

Figure 3. Comparison of mesh models with different cell shapes

Table 1. Boundary conditions for calculating the turbocharger impellers

Angular speed, rpm	Parameter	Inlet		Outlet	
		Turbine	Compressor	Turbine	Compressor
48,000	Pressure, Pa	134,762	101,325	101,325	147,934
	Temperature, K	918	300	828	340
57,000	Pressure, Pa	151,987	101,325	101,325	175,292
	Temperature, K	920	306	829	370
67,000	Pressure, Pa	172,252	101,325	101,325	202,650
	Temperature, K	930	308	838	391
76,000	Pressure, Pa	200,623	101,325	101,325	243,180
	Temperature, K	926	301	808	407
86,000	Pressure, Pa	230,007	101,325	101,325	290,802
	Temperature, K	925	306	794	444
95,000	Pressure, Pa	263,445	101,325	101,325	356,664
	Temperature, K	926	308	796	482

Table 2. Physical properties of flue gases

Temperature T, °C	Density ρ, kg/m^3	Heat capacity C_p, J/kgK	Thermal conductivity λ, W/mK	Dynamic viscosity μ, Pas
273	1.295	1042	0.0228	1.58×10^{-5}
373	0.950	1068	0.0313	2.04×10^{-5}
473	0.748	1097	0.0401	2.45×10^{-5}
573	0.617	1122	0.0484	2.82×10^{-5}
673	0.525	1151	0.0570	3.17×10^{-5}
773	0.457	1185	0.0656	3.48×10^{-5}
873	0.405	1214	0.0742	3.79×10^{-5}
973	0.363	1239	0.0827	4.07×10^{-5}

Table 3. Physical properties of dry air

Temperature T, °C	Density ρ, kg/m^3	Heat capacity C_p, J/kgK	Thermal conductivity λ, W/mK	Dynamic viscosity μ, Pas
273	1.293	1005	0.0244	1.72×10^{-5}
373	0.946	1009	0.0321	2.19×10^{-5}
473	0.746	1026	0.0393	2.60×10^{-5}
573	0.615	1047	0.0460	2.97×10^{-5}
673	0.524	1068	0.0521	3.30×10^{-5}
773	0.456	1093	0.0574	3.62×10^{-5}
873	0.404	1114	0.0622	3.91×10^{-5}
973	0.362	1135	0.0671	4.18×10^{-5}

In the calculation, the energy equation was used to describe the variable temperature field, and the SST k-ω turbulence model was applied [26]. Turbulent parameters were set through the turbulence intensity and hydraulic diameter.

The simulation of the gas dynamics of the impellers resulted in certain pressure fields, temperature fields and velocity components. An example of the results obtained for the 95,000 rpm mode is shown in Figure 4. The temperature fields turned out to be more uniform, so their visual presentation is uninformative. The temperature fields are then imported into the steady-state thermal module for coupled thermal calculations.

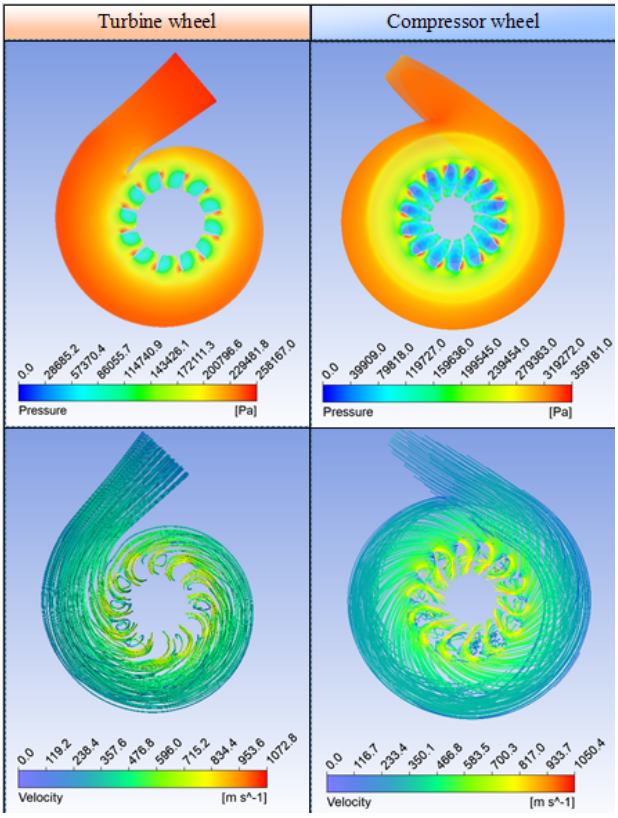

Figure 4. Pressure fields and velocity vectors for 95,000 rpm

2.3 Selection of materials

For each element of the TCR assembly, the appropriate material was selected. The materials of the parts are presented in Table 4. The functions of thermal conductivity of materials on temperature, taken from the literature [27-30], are presented in Figure 5.

Table 4. Materials of turbocharger assembly parts

Detail	Material
Rotor shaft, thrust washers, distance rings, sealing rings	Steel 40X (EN 37Cr4KD)
Bearing housing, turbine housing	Cast iron ВЧ40 (EN-GJS-400-15)
Turbine wheel	Heat resistant nickel alloy Rene 41
Radial bearing, thrust bearing	Bronze БрОС10-10 (UNS C93700)
Oil sump screen, oil deflector, rear wall, turbine screen	Stainless steel 12X18H10T (EN 1.4878)
Compressor wheel, compressor housing	Aluminium АЛ4 (UNS A13600)

2.4 Calculation of the heat transfer coefficient

The final step in the thermal calculation is to determine the heat transfer coefficient. The function of heat exchange between the TCR body and the ambient air was taken from the ANSYS library. To determine the heat transfer coefficient of the lubricant, a computational model of the oil system was developed. The axial bearing geometry has been simplified for a higher quality mesh model. Heat transfer between the engine and the turbocharger casing was not considered. The computational model was divided into four parts (Fig. 6). Due to this, the heat transfer coefficient could be determined locally to take into account the behaviour of the flow.

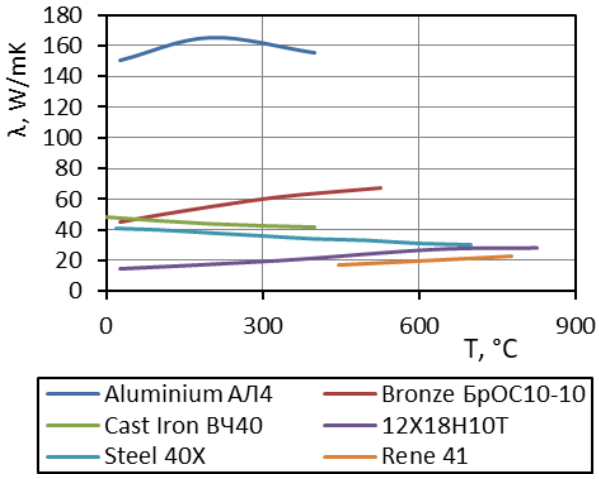

Figure 5. Change in thermal conductivity of materials from temperature

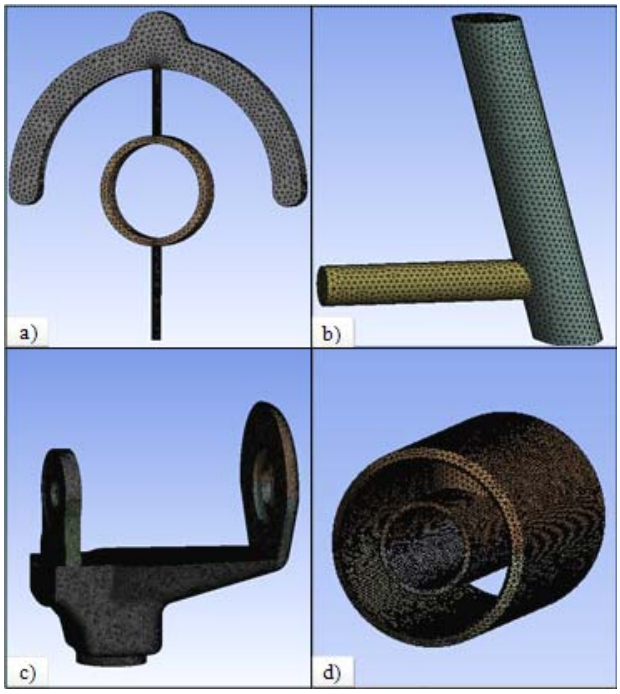

Figure 6. Control units of the design model of the lubrication system: (a) thrust bearing, (b) input line, (c) bearing housing and (d) radial bearing

The initial temperature of the turbocharger elements was equivalent to 22 °C. The heat flux density was set from two sides of the main heat

sources: the turbine housing and the compressor. The pressure at the inlet to the lubrication system was 400 kPa, and at the outlet 101 kPa. The oil temperature at the inlet was 90 °C, and at the outlet 110 °C. Mineral oil SAE 40 was used for modelling. The physical properties of the lubricant are indicated in Table 5. The values of the heat transfer coefficients at different operating modes for each unit of the lubrication system are shown in Figure 7. The dependence of the heat transfer coefficient between the TCR housing and external air is shown in Figure 8.

Based on the results obtained, it can be concluded that with an increase in the rotor speed, the value of the heat transfer coefficient most significant increases is in the radial bearing assembly. In other units, it increases by 0.3 – 8 % of the initial value, depending on the rotor speed. The obtained values of the heat transfer coefficient were used to determine the temperatures in the TCR housing.

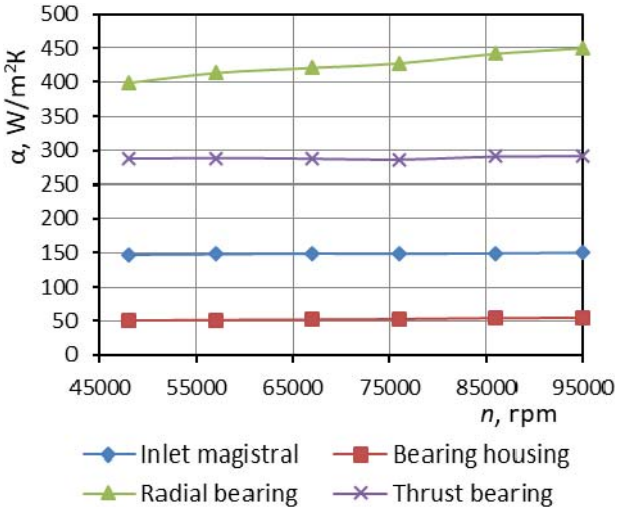

Figure 7. The heat transfer coefficients value at different operating modes for the lubrication system control units

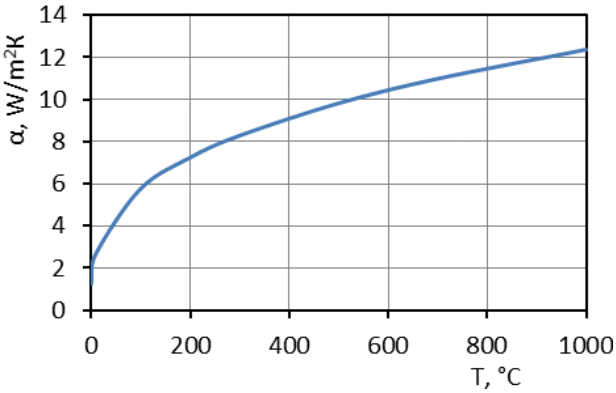

Figure 8. The function of convective heat exchange between the TCR body and external air

3. Results

3.1 Simulation of temperature fields in the clearances of the bearing assembly

The result of the simulation was the determination of the values of temperatures (Table 6) and thermal fields. Thermal fields in the bearing housing are presented in a previous work [31]. The obtained data testify to the uneven heating of the bearings and the rotor. The range of temperature difference in the inner layer can be 19.5 – 55 °C. This is logical considering that the rotor is the main heat transfer from the turbine to the compressor. The range of temperature difference in the outer layer can be 6.5 – 42.5 °C. With a decrease in the rotor speed, the temperature difference tends to the maximum value. The airflow rate in the turbine and compressor housings is reduced. In the turbine housing, this leads to an increase in gas temperature due to a decrease in the rate of heat transfer. The opposite situation is observed in the compressor housing. The average air temperature decreases due to the pressure drop, which affects the air compression process.

Table 5. Physical properties of engine oil

Temperature T, °C	Density ρ, kg/m^3	Heat capacity C_p, J/kgK	Thermal conductivity λ, W/mK	Dynamic viscosity μ, Pas
90	857.30	2152.1	0.12	0.0080
95	854.24	2172.5		0.0074
100	851.17	2192.9		0.0068
105	848.11	2213.3		0.0063
110	845.04	2233.7		0.0058
115	841.98	2254.1		0.0054
120	838.91	2274.5		0.0051
125	835.85	2294.9		0.0048
130	832.78	2315.3		0.0045

Table 6. Engine oil temperature in the gaps under different operating modes

Rotation frequency *n*, rpm	Engine oil temperature, °C			
	Internal clearance from the turbine side	Internal clearance from the compressor side	External clearance from the turbine side	External clearance from the compressor side
48,000	127.6	72.8	124.3	81.9
57,000	125.0	78.8	122.1	88.2
67,000	126.1	84.1	123.3	93.8
76,000	124.7	87.2	122.1	97.2
86,000	123.3	95.0	121.0	105.5
95,000	123.2	103.7	121.3	114.8

Table 7. Comparison of the results with the works of other authors

Author	*n*, rpm	Location	Engine oil temperature, °C		The results obtained by the authors, °C
			Modelling	Experiment	
Lushcheko et al. (2017)	100,000	external clearance turbine	109 – 112	115 – 133	121
		external clearance compressor	104 – 105	113 – 116	115
Li et al. (2017)	50,000 – 100,000	external clearance turbine	142 – 156	150 – 155	121 – 124
		external clearance compressor	118 – 122	111 – 121	82 – 115
		internal clearance turbine	155 – 184	–	123 – 128
		internal clearance compressor	118 – 135	–	73 – 104
Zadorozhnaya et al. (2017)	90,000	oil drain from the turbine side	107 – 122	109 – 111	123
		oil drain from the compressor side	97 – 112	103 – 104	104
			Full fuel experiment	Idling experiment	
Khanin et al. (1991)	60,000	external clearance turbine	147 – 167	127 – 132	122
		external clearance compressor	147 – 277	107 – 137	125

3.2 Verification of results

Verification of the results was carried out based on a comparison with the results obtained by other authors.

Research [17] is devoted to the study of thermohydrodynamic (THD) characteristics of a turbocharger rotor bearing system using numerical modelling and experiments. In the experiments, the gas was heated to 600 °C. This temperature was maintained during the acceleration of the rotor to 24,000 rpm. The lubricant supply temperature was 100 °C and the oil supply pressure was 4 bar. The authors managed to determine the temperature values in the external and internal bearing clearances, as well as to plot the dependence on the rotor speed.

In the article [32], the boundary conditions for modelling and experiment corresponded to the operation of the TCR 7 turbocharger in the nominal model of a diesel engine with a power of 270 kW. The gas flow rate through the turbine is 0.2 kg/s at a temperature of 650 °C. The air pressure at the compressor outlet from the compressor is 220 kPa at a flow rate of 0.2 kg/s and a temperature of 200 °C. The oil feed temperature was equivalent to 100 °C at a pressure of 500 kPa. Rotor speed is 100,000 rpm. The simulation results are in good agreement with the experimental results. The temperature difference in the external clearance between the turbine and compressor bearings is 2 – 17 °C. The design of the TKR presented in the work is the closest to the turbocharger considered in this article.

Khanin et al. [33] in their work presented the results of tests of a turbocharger on a non-motorized stand. Changes in the temperature of the lubricant and individual points of the bearing housing were investigated as a function of the rotor speed, gas temperature and lubricant consumption. The temperature of the gases in the turbine housing reached 700 degrees. Temperature measurements were carried out at a rotor speed from 30,000 to 60,000 rpm, as well as after

stopping the engine operating in full oil supply or idling. Temperature values were measured within 15 minutes after the engine was turned off.

In the work [23], the calculation of hydrodynamic phenomena in a journal bearing was carried out taking into account the dynamics of a flexible rotor of a turbocharger. The object of the study was TCR 50. The rotor speed ranged from 84,500 to 186,000 rpm. The oil supply pressure was varied from 140 to 400 kPa, and the oil temperature at the inlet to the bearing housing was taken from 70 to 105 °C. At an oil supply pressure of 400 kPa and a lubricant temperature of 90 °C, the temperature inside the bearing varied from 105 to 117 °C, depending on the rotor speed. At a speed of 90,000 rpm, the temperature difference between the bearings of the turbine and the compressor was about 7 – 10 °C. A more detailed comparison of the results obtained with the works of other authors is presented in Table 7.

Based on the comparison made, it can be concluded that despite the difference in design, materials and values of the parameters of working processes, the obtained temperature values are adequate and correspond to the ranges presented in the works of other authors.

3.3 Modelling the deformed state of bearing parts

The deformation of the parts of the TCR bearing assembly occurs under the influence of pressure forces, centrifugal forces and temperature differences. Small radial loads from the side of the rotor, and the hardness of the materials of the friction pairs make it possible to neglect mechanical deformations in most cases [34]. Thermal deformations of the elements of the bearing assembly, in turn, can lead to significant changes in the values of the clearances in the TCR bearings with increasing temperature. Therefore, for the obtained values of temperatures and thermal fields, a strength analysis was carried out in order to determine the values of the deformations of the bearing elements under the influence of temperatures.

The calculation of the deformed state was carried out in the ANSYS static structural module. The rotor was fixed in all directions except radial. Fastening took place in the areas of the seals so as not to affect the amount of deformations in the bearing clearances. The sleeve was only secured axially from the axial bearing side. Figure 9 shows the fixing scheme of the design “sleeve-rotor model” (the places for fixing the rotor are highlighted in blue, and the places for fixing the sleeve are highlighted in yellow). The deformations of the bearing housing were not taken into account in the calculation.

Figure 9. Scheme of fastening of the design “sleeve-rotor” model

The bushing material is bronze БрОС10-10 with Poisson's ratio of 0.35, and the rotor material is steel 40X with Poisson's ratio of 0.3. The rest of the mechanical properties of materials are presented in Table 8 [35,36].

Table 8. Mechanical properties of bushing and rotor materials

Material	Temperature, °C	Thermal expansion coefficient, 1/°C	Young's modulus, GPa
Steel 40X	20	–	214
	100	1.19×10^{-5}	211
	200	1.25×10^{-5}	206
	300	1.32×10^{-5}	203
	400	1.38×10^{-5}	185
	500	1.41×10^{-5}	176
	600	1.44×10^{-5}	164
	700	1.46×10^{-5}	143
Bronze БрОС10-10	–	1.82×10^{-5}	110

According to the simulation results, the expansion of the elements of the bearing assembly in the radial direction was observed, and the difference in local temperatures of the elements leads to their uneven deformation along the diameter (Fig. 10). Changed clearances under the influence of thermal deformations are presented in Table 9.

The trend in thermal expansion clearances is identical to that in temperatures. The maximum values of thermal deformations on the turbine side are observed at a rotation speed of 48,000 rpm, and on the compressor side at 95,000 rpm. It can be seen from the results that the change in the internal clearance due to the expansion of the rotor is compensated by the expansion of the

sleeve, due to which the clearance changes insignificantly (0.3 – 0.8 % from the initial value). In the case of an external clearance, its value changes more significantly (0.6 – 8.3 % from the initial value), but it should be taken into account that the calculation did not take into account the expansion of the bearing housing.

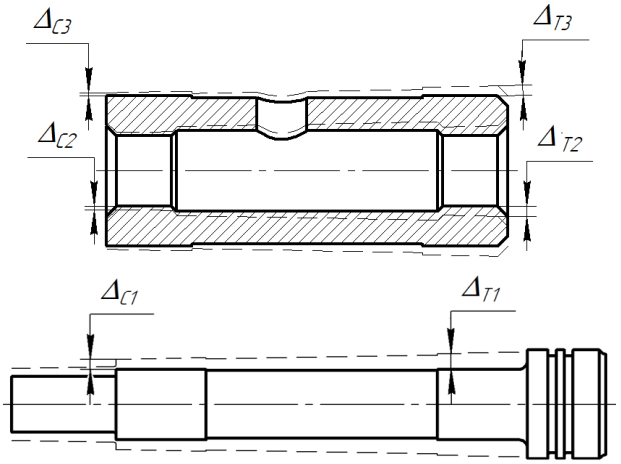

Figure 10. Deformation of the bushing and rotor shaft (—— cold state; ---- hot state)

Table 9. Changed clearances under the influence of thermal deformations

n, rpm	Turbine clearance, µm		Compressor clearance, µm	
	internal	external	internal	external
95,000	29.92	55.32	30.24	59.33
86,000	29.91	55.26	30.22	59.42
76,000	29.91	55.17	30.21	59.51
67,000	29.91	55.10	30.16	59.54
57,000	29.90	55.13	30.20	59.59
48,000	29.90	55.01	30.19	59.64

With the help of the developed software [23], hydrodynamic calculation of bearings and dynamics of a flexible rotor was carried out for two cases: 1 – without taking into account thermal deformations; 2 – taking into account the obtained values of thermal deformations. When calculating the dynamics of the rotor at a speed of 95,000 rpm, taking into account the change in the clearances of the working units, the following factors were identified:

- Case 2 has a higher total friction loss. They increased by 1.47 %.
- The highest pressure values are observed in Case 2 from 1 to 4.57 MPa. This is due to the higher vibration amplitude of the rotor. It is 2 – 9 % larger than Case 1, depending on the selected clearance.
- The vibration amplitude of the impellers changed insignificantly. In Case 2, the values of the wheel amplitudes are 3 % higher than in Case 1.

As a result, it can be concluded that changes in the clearances under the influence of thermal expansion adversely affect the operation of the turbocharger, leading to an increase in the amplitude of oscillations. This phenomenon must be taken into account when developing modern mechanisms and machines. A comparison of the vibration amplitudes of the impellers, bearings and rotor, presented in micrometres, in the radial direction is shown in Figure 11.

4. Conclusions

The article presented an algorithm for calculating heat transfer in the turbocharger bearing housing. As a result of the calculation, the thermal fields in the bearing housing, the values of

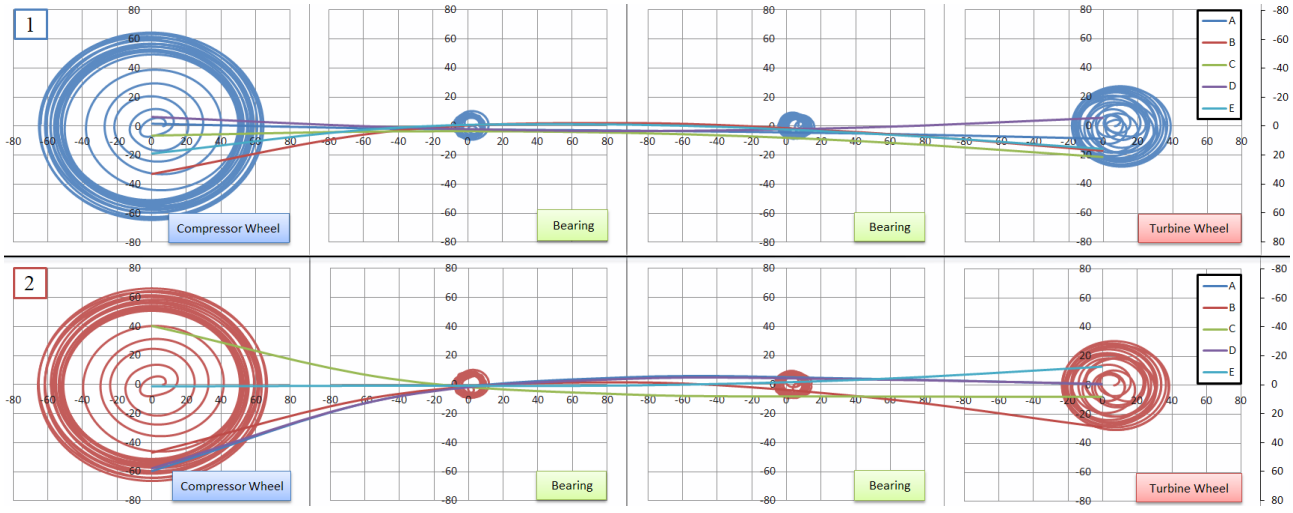

Figure 11. Comparison of the vibration amplitudes of the impellers, bearings and rotor in radial direction (1 – excluding thermal expansion of parts; 2 – taking into account the thermal expansion of parts)

temperatures in the external and internal clearance of the bearing, as well as the values of the change in the clearances under the influence of the thermal expansion of the parts were obtained. The data obtained were verified with the results presented in the work of other authors, and indicate the uneven thermal loading of the radial bearing. This factor has a significant impact on the hydromechanical characteristics of the support unit, and hence on the durability of the turbocharger. Based on the results obtained, the following conclusions were made:

- The highest value of the heat transfer coefficient is observed in the radial bearing of the turbocharger. With an increase in the rotor speed, the heat transfer coefficient increases by 3.7 – 13 % of the initial value. In other nodes, the growth reaches from 0.3 to 8 %, depending on the operating mode.
- The range of temperature difference in the inner layer can be 19.5 – 55 °C and in the outer layer can be 6.5 – 42.5 °C, depending on the rotor speed.
- The change in the internal clearance due to the expansion of the rotor is compensated by the expansion of the bushing, due to which the clearance changes slightly (0.3 – 0.8 %). In the case of an external clearance, its value changes more significantly (0.6 – 8.3 %), but it should be taken into account that the calculation did not take into account the expansion of the bearing housing. This requires clarification of the results in further studies.
- The heat-deformed version has higher total friction losses. They increased by 1.47 %.
- The highest pressure values are observed in Case 2 from 1 to 4.57 MPa. This is due to the higher vibration amplitude of the rotor. It is 2 – 9 % larger than Case 1, depending on the selected clearance.
- The vibration amplitude of the impellers changed insignificantly. In Case 2, the values of the wheel amplitudes are 3 % higher than in Case 1.

The presented algorithm combines three numerical methods that underlie the commercial software developed by the authors. This combination allows solving complex conjugate problems and levelling the disadvantages of the methods due to their joint use. Such algorithms are necessary when the requirements for the development of modern technology increase and they allow achieving a larger amount of output data.

The developed algorithm will be used to calculate the rotor dynamics and optimize the bushing design in order to increase the reliability and durability of the bearing assembly when designing new generation turbochargers.

Acknowledgement

The work was carried out with the financial support of the Russian Foundation for Basic Research (project No. 20-48-740007 \ 20).

References

[1] Turbocharger market, available at: https://www.alliedmarketresearch.com/turbocharger-market, accessed: 11.04.2022.

[2] T. Dziubak, M. Karczewski, Operational malfunctions of turbochargers – reasons and consequences, Combustion Engines, Vol. 164, No. 1, 2016, pp. 13-21, DOI: 10.19206/CE-116484

[3] Why do turbochargers fail? available at: https://www.garrettmotion.com/ru/news/newsroom/article/why-do-turbochargers-fail/#:~:text=Most%20failures%20are%20caused%20by,fitting%20usually%20causes%20oil%20starvation, accessed: 11.04.2022.

[4] A. Romagnoli, R. Martinez-Botas, Heat transfer on a turbocharger under constant load points, in Proceedings of the ASME Turbo Expo 2009: Power for Land, Sea, and Air, Volume 5, 08-12.06.2009, Orlando, Florida, USA, pp. 163-174, DOI: 10.1115/GT2009-59618

[5] D. Deng, F. Shi, L. Begin, I. Du, The effect of oil debris in turbocharger journal bearings on subsynchronous NVH, SAE Technical Paper Series, 2015, Paper 2015-01-1285, DOI: 10.4271/2015-01-1285

[6] Q. Hu, M. Zhu, J. Yang, Study on thermal unstable vibration of rotor under journal whirl with large amplitude in journal bearing, International Journal of Rotating Machinery, Vol. 2020, 2020, Paper 1980759, DOI: 10.1155/2020/1980759

[7] J.A. Lorenz, B.T. Murphy, Case study of Morton effect shaft differential heating in a variable-speed rotating electric machine, in Proceedings of the ASME 2011 Turbo Expo: Turbine Technical Conference and Exposition, Volume 6, 06-10.06.2011, Vancouver, Canada, pp. 257-269, DOI: 10.1115/GT2011-45228

[8] X. Tong, A. Palazzolo, Measurement and prediction of the journal circumferential temperature distribution for the rotordynamic Morton effect, Journal of Tribology, Vol. 140, No. 3, 2018, Paper 031702, DOI: 10.1115/1.4038104

[9] D. Polichronis, R. Evaggelos, G. Alcibiades, G. Elias, P. Apostolos, Turbocharger lubrication – Lubricant behavior and factors that cause turbocharger failure, International Journal of Automotive Engineering and Technologies, Vol. 2, No. 1, 2013, pp. 40-54.

[10] J.R. Serrano, A. Tiseira, L.M. García-Cuevas, T. Rodríguez Usaquén, Adaptation of a 1-D tool to study transient thermal in turbocharger bearing housing, Applied Thermal Engineering, Vol. 134, 2018, pp. 564-575, DOI: 10.1016/j.applthermaleng.2018.01.085

[11] A.M. Plaksin, A.V. Gritsenko, A.Y. Burtsev, K.V. Glemba, K.I. Lukomsky, Extending the life of turbochargers automotive engineering application of the accumulator in the lubrication system, Fundamental research, Vol. 6, No. 4, 2014, pp. 728-732.

[12] S. Shaaban, Experimental Investigation and Extended Simulation of Turbocharger Non-adiabatic Performance, PhD thesis, Leibniz University Hannover, Hanover, 2004, DOI: 10.15488/6456

[13] N. Baines, K.D. Wygant, A. Dris, The analysis of heat transfer in automotive turbochargers, Journal of Engineering for Gas Turbines and Power, Vol. 132, No. 4, 2010, Paper 042301, DOI: 10.1115/1.3204586

[14] M. Cormerais, J.F. Hetet, P. Chesse, A. Maiboom, Heat transfer analysis in a turbocharger compressor: Modeling and experiments, SAE Technical Paper Series, 2006, Paper 2006-01-0023, DOI: 10.4271/2006-01-0023

[15] R.D. Burke, P. Olmeda, F.J. Arnau, M. Reyes-Belmonte, Modelling of turbocharger heat transfer under stationary and transient engine operating conditions, in 11th International Conference on Turbochargers and Turbocharging, 13-14.05.2014, London, UK, pp. 103-112, DOI: 10.1533/978081000342.103

[16] O. Willers, J.R. Seume, C. Zeh, H. Schwarze, Thermal influence on the overall TC system with consideration of the coupled bearings, MTZ worldwide, Vol. 82, No. 2, 2021, pp. 56-60, DOI: 10.1007/s38313-020-0609-8

[17] Y. Li, F. Liang, Y. Zhou, S. Ding, F. Du, M. Zhou, J. Bi, Y. Cai, Numerical and experimental investigation on thermohydrodynamic performance of turbocharger rotor-bearing system, Applied Thermal Engineering, Vol. 121, 2017, pp. 27-38, DOI: 10.1016/j.applthermaleng.2017.04.041

[18] I.A. Suvorov, L.A. Berdnikov, Исследование возможности тепловой оптимизации ротора турбокомпрессора с проведением конечно-элементных анализов [Study the possibility of thermal optimization of turbocharger rotor with carrying out finite element analisis], Труды Нижегородского государственного технического университета им. Р.Е. Алексеева, Vol. 78, No. 4, 2013, pp. 56-65 [in Russian].

[19] H. Aghaali, H.-E. Ångström, J.R. Serrano, Evaluation of different heat transfer conditions on an automotive turbocharger, International Journal of Engine Research, Vol. 16, No. 2, 2015, pp. 137-151, DOI: 10.1177/1468087414524755

[20] H. Aghaali, H.-E. Ångström, Turbocharged SI-engine simulation with cold and hot-measured turbocharger performance maps, in Proceedings of the ASME Turbo Expo 2012: Power for Land, Sea, and Air, Volume 5, 11-15.06.2012, Copenhagen, Denmark, pp. 671-679, DOI: 10.1115/GT2012-68758

[21] T. Helmig, R. Kneer, A novel transient infrared-thermography based experimental method for the inverse estimation of heat transfer coefficients in rotating bearings, International Journal of Thermal Sciences, Vol. 167, 2021, Paper 107000, DOI: 10.1016/j.ijthermalsci.2021.107000

[22] A. Romagnoli, A. Manivannan, S. Rajoo, M.S. Chiong, A. Feneley, A. Pesiridis, R.F. Martinez-Botas, A review of heat transfer in turbochargers, Renewable and Sustainable Energy Reviews, Vol. 79, 2017, pp. 1442-1460, DOI: 10.1016/j.rser.2017.04.119

[23] E. Zadorozhnaya, S. Sibiryakov, V. Hudyakov, Theoretical and experimental investigations of the rotor vibration amplitude of the turbocharger and bearings temperature, Tribology in Industry, Vol. 39, No. 4, 2017, pp. 452-459, DOI: 10.24874/ti.2017.39.04.04

[24] B.A. Sharoglazov, V.V. Shishkov, Reciprocating Engines: Theory, Modeling, and Calculation of Processes, Publishing Centre SUSU, Chelyabinsk, 2011.

[25] M.A. Mikheev, I.M. Mikheeva, Basics of Heat Transfer, Energy, Moscow, 1977.

[26] F.R. Menter, Influence of freestream values on *k-ω* turbulence model predictions, AIAA Journal, Vol. 30, No. 6, 1992, pp. 1657-1659, DOI: 10.2514/3.11115

[27] V.M. Beletsky, G.A. Krivov, Aluminium alloys. Composition, Properties, Technology, Applications, Kominteh, Kiev, 2005.

[28] V.V., Gerasimov and A.S., Monachov Materials of Nuclear Technology, Energoatomizdat, Moscow, 1982.

[29] René 41, available at: https://www.rolledalloys.com/alloys/cobalt-alloys/rene-41/en, accessed: 11.04.2022.

[30] V.S. Chirkin, Thermophysical Properties of Materials for Nuclear Technology, Energoatomizdat, Moscow, 1967.

[31] E. Zadorozhnaya, V. Hudyakov, E. Polyacko, I. Dolgushin, Modelling the thermal state of a turbocharger bearing housing when calculating the rotor dynamics at transient modes, Industrial Lubrication and Tribology, Vol. 74, No. 3, 2022, pp. 342-349, DOI: 10.1108/ILT-06-2021-0215

[32] V.A. Lushcheko, R.R. Khasanov, A.K. Khairullin, V.M. Gureev, Исследование работы элементов турбокомпрессора двигателя внутреннего сгорания [Research into the operation of turbocharger components in an internal combustion engine], No. 12, 2017, pp. 20-29, DOI: 10.18698/0536-1044-2017-12-20-29 [in Russian].

[33] N.S. Khanin, E.V. Aboltin, B.F. Lyamtsev, Automobile Engines with Turbocharging, Mechanical Engineering, Moscow, 1991.

[34] N.A. Raykovskiy, V.L. Yusha, A.V. Tretyakov, V.A. Zakharov, K.I. Kuznetsov, The method for studying temperature deformations of self-lubricating bearing friction units of high-temperature low-flow turbine, Omsk Scientific Bulletin. Series «Aviation-Rocket and Power Engineering», Vol. 3, no. 2, 2019, pp. 51-61, DOI: 10.25206/2588-0373-2019-3-2-51-61

[35] A.V. Darkov, G.S. Shpiro, Resistance of Materials, Higher School, Moscow, 1989.

[36] N.G. Kuklin, G.S. Kuklina, Machine Parts, Higher School, Moscow, 1987.